

Non-Reciprocity in an Active Two-Dimensional Lattice Circuit

Justin White

Defense Date: April 3, 2019

Research Advisor:	Konrad Lehnert	Dept. of Physics
Honors Council Representative:	Paul Beale	Dept. of Physics
Third Party Committee Member:	Agnès Beaudry	Dept. of Mathematics

Abstract

Circulators are crucial components in quantum computers that ensure that quantum information is coherently transported. Current commercial circulators are too bulky because they use permanent magnets, so producing chip-scale circulators is necessary to feasibly scale up the size of quantum computers using superconducting qubits. Using a model inspired by a paper by Rudner [2], I have designed a lattice circuit that will produce non-reciprocity, which is the property required for proper circulation. These lattice circuits are able to produce circulation because they have periodically time-dependent bonds that control interactions between the sites in the lattice. In this thesis, I first theoretically analyze two similar lattice circuits and show that they can both produce non-reciprocity. Finally, I experimentally demonstrate non-reciprocity in a 2 by 2 lattice circuit at room temperature. This experimental verification of circulation motivates future testing of larger lattices and building superconducting versions of the circuit to create chip-scale circulators.

Contents

1	Introduction	3
2	Theory	6
A	Circuit One: Lattice Circuit with Sites as Capacitors	6
i	Solving the Unit Cell of the Lattice Circuit	7
ii	Solving the Entire Lattice Circuit	10
B	Circuit Two: Lattice Circuit with Sites as Capacitors and Induc- tors in Parallel	12
i	Solving the Unit Cell of the Lattice Circuit	12
ii	Solving a 2 by 2 Circuit	15
3	Experiment	17
A	Testing the Unit Cell for Circuit Two	17
B	Experimental Setup for 2 by 2 Version of Circuit Two	18
C	Testing a 2 by 2 Version of Circuit Two for Non-Reciprocity	21
4	Conclusion	27
5	Appendix	28
A	Circuit One: Solution to Unit Cell	28
B	Circuit One: Equations of Motion	29
C	Circuit Two: Solution to Unit Cell	30
D	Optimization of Coupling Parameter	32
E	Datasheet for SRA-6+ Frequency Mixer	33

1 Introduction

Circulators are crucial components in quantum computers that ensure qubit coherence as the qubit's information is transported. The quantum information is contained in a voltage signal that is read out from the qubit, and it is important to be able to shield this voltage signal from external influences. Circulators are multiple port devices that directionally transmit signals such that signals starting in port i end in port $i + 1$ [1]. Consequently, the quantum information stored in the voltage signal can be transmitted to later ports to be processed without the electronics at those ports affecting the signal before it arrives. The current commercial circulators are too bulky to feasibly scale up the number of superconducting qubits in a quantum computer because the circulators rely on large permanent magnets that are difficult to integrate with superconducting qubits [1]. In contrast, the small size of chip-scale circulators makes them an attractive option to overcome the scaling issue that current commercial circulators present. One goal of my research is to test a circuit at room temperature to see if it has the potential to create circulation as a chip-scale circulator.

The specific design of the circuit that will achieve non-reciprocity is inspired by a paper written by Rudner et al [2]. This paper in the field of theoretical condensed matter physics describes a way to create robust chiral edge modes (i.e. non-reciprocity) in a lattice even if the Chern number is 0 for all the bulk Floquet band gaps. This phenomenon is interesting because, for a static Hamiltonian, the Chern number for a bulk band gap quantifies how many chiral edge modes there are. A Chern number of 0 usually means that there are not any chiral edge modes; however, the inclusion of time dependence in the Hamiltonian, which is what creates bulk Floquet band gaps, produces chiral edge modes even if the Chern number is 0 [2]. The resulting non-reciprocity from a time-dependent lattice relates to circulators because this type of lattice has robust chiral edge modes that do not excite the bulk of the lattice. Having an excitation on the edge of the lattice that travels in only one direction around the lattice and which does not decay to the bulk is how we want the voltage signals to behave in a circulator. Since the circulation produced by a circulator and the non-reciprocity of a lattice are such similar properties, I will use them interchangeably hereafter.

Creating a non-reciprocal lattice requires particular types of time dependence in the lattice. Figure 1a shows a modified image from Rudner's paper depicting what such time dependence looks like. In this lattice, there are two

different types of sites denoted by white and black dots. There are also four different types of bonds in the lattice, and those types of bonds are turned off and on at the same rate but with four different phases. At any one time there is only one type of bond on, which means that a site is either connected to only one adjacent site or not connected to any sites.

Figure 1b depicts examples of how excitations in the lattice progress over time. Depending on the order of the bond switching, excitations initialized on the boundary will travel clockwise or counterclockwise and excitations initialized in the bulk will travel in the opposite direction as those on the boundary. For instance, the green path shown in Figure 1b begins with an excitation on a white site on the top edge of the lattice. During the first part of the cycle, the white site can interact with the black site to its left. During this interaction the excitation transfers to the black site, and then the second part of the cycle begins. In this part of the cycle, the excitation cannot interact with any sites around it, so nothing happens. Finally, in the third part of the cycle the excitation can transfer to the white corner site. Though not shown, this excitation will continue to travel around the edge of the lattice counterclockwise. This model thus produces the results that we desire for a non-reciprocal device like a circulator. So, we will use this model laid out by Rudner as an inspiration for designing a non-reciprocal active (i.e. time-dependent) two-dimensional lattice circuit.

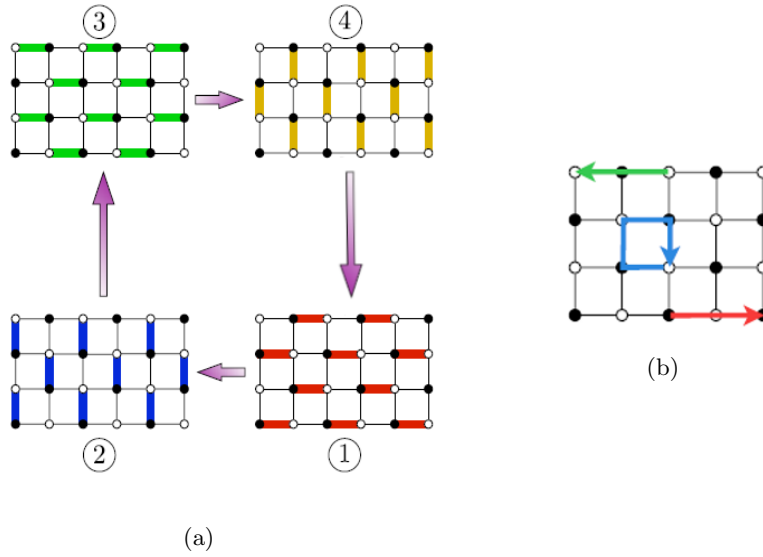


Figure 1: (a) The lattice has two different types of sites denoted by black and white dots, and it has four different types of bonds represented by four different colors (red, blue, green, and yellow). The purple arrows demonstrate a bond switching scheme for the lattice that produces circulation. During each part of the cycle (1, 2, 3, and 4) only one color of bond is activated (i.e. interactions between sites connected by a colored bond are allowed). (b) These are examples of how excitations propagate through the circuit given different starting points on the lattice. Excitations initialized on the boundary will travel counterclockwise and excitations initialized in the bulk will travel clockwise because of the particular switching scheme used and shown in Figure 1a.

2 Theory

A Circuit One: Lattice Circuit with Sites as Capacitors

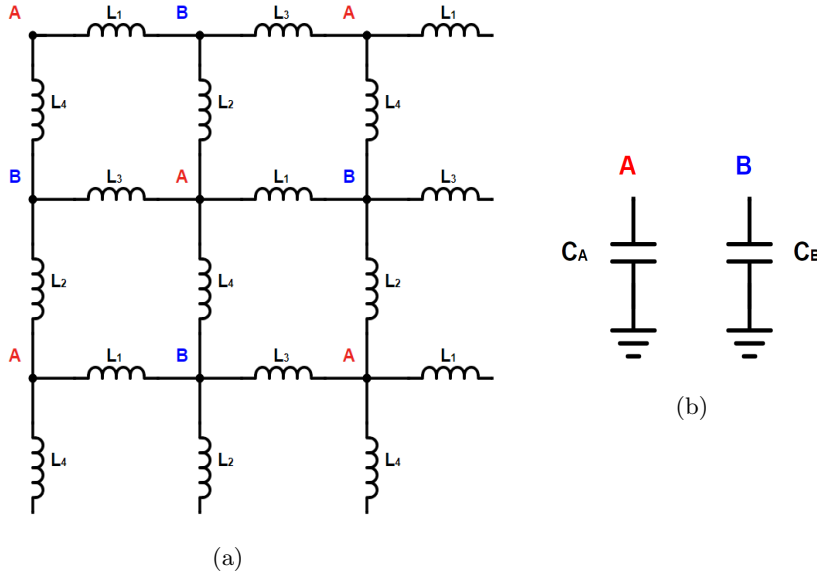


Figure 2: (a) This is a circuit diagram for circuit one. Each node in the circuit is a lattice site (A or B), and the sites are connected to each other by coupling inductors with inductances L_1 , L_2 , L_3 , and L_4 . (b) The A and B sites are capacitors to ground with capacitances C_A and C_B .

Inspired by Rudner’s bond switching model, we designed a circuit that would implement the lattice he describes. The sites of the lattice are capacitors that can store electrical energy when they accrue charge and thus a voltage drop across them. The bonds of the lattice are inductors, and when two capacitors are connected to an inductor they will interact by periodically exchanging voltage. Figure 2 shows circuit diagrams for this lattice of capacitor sites and coupling inductor bonds. Throughout the rest of this paper, I will refer to this circuit design as circuit one. Figure 2a shows circuit one, which consists of A and B sites coupled by four different types of inductors. Figure 2b shows that the A and B sites are grounded capacitors. Even if the capacitances of the A and B site capacitors are the same, these sites can be distinguished by which type of inductors surround them. There are four different inductor types numbered 1 through 4, and these appear in different orders around a site depending on if it

is an A or a B site.

Though not shown in Figure 2, we know that a non-idealized version of this circuit should account for the equivalent series resistance of the coupling inductors. The effect of these resistances will be addressed in the following section when we analyze the unit cell of circuit one. Presently, we have only discussed passive elements in circuit one; however, achieving non-reciprocity requires introducing time dependence in the circuit. One way to simulate time dependence in circuit one is to modulate the coupling inductors between some reasonable finite value and an infinite value. In practice, we will not be able to modulate inductance at the high frequencies this will require; however, the simulation can modulate inductance this quickly and I will discuss how to experimentally modulate bonds in a future section. A reasonable finite value simulates a bond that allows sites to interact with each other, while an infinite value simulates a bond that does not allow sites to interact with each other. Crucially, though, we need to know for what periods of time the bond should and should not allow interaction. To determine these periods, we need to understand how the voltage exchanges in the unit cell of circuit one.

i Solving the Unit Cell of the Lattice Circuit

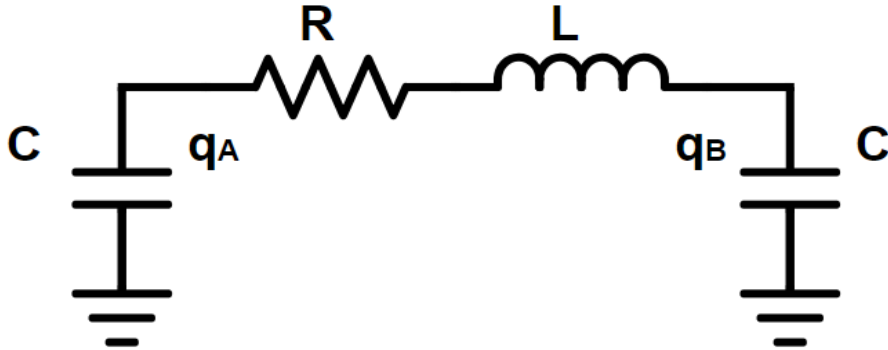


Figure 3: This is the unit cell of circuit one in which two sites are connected by a bond and are disconnected from any other sites. All of the A and B sites have identical capacitors with capacitance C and the coupling inductors are all identical with inductance L . In addition, the equivalent series resistance of each coupling inductor is represented by a resistor with resistance R .

When voltage exchanges between two sites, the large lattice circuit simplifies

to a unit cell shown in Figure 3 because each site can only interact with one other site. Once the bond between two sites allows interaction, it needs to maintain this interaction until all the charge has transferred from one site to the next. The amount of time it takes for the charge to transfer from one site to the next is called the bond switching time. We will solve for how the charge changes on the site capacitors as a function of time to determine the proper bond switching time.

A charge q_0 is initialized on only one of the capacitors, and then we want to determine when the charge transfers fully to the other capacitor. Resistance is included in the circuit shown in Figure 3 because it will be important to see if the inductor's equivalent series resistance significantly affects the bond switching period. In the circuit diagram, q_A is the charge on site A , q_B is the charge on site B , R is the equivalent series resistance of the inductor, each capacitor has capacitance C , and the coupling inductor has inductance L . Appendix A details the derivation of the solution for the charges on the capacitors, and the equation of motion it solves is

$$\ddot{q}_A + \frac{R}{L}\dot{q}_A + \frac{1}{LC}q_A = \frac{q_0}{LC}. \quad (1)$$

After solving and reparameterizing equation 1, the solution for the charge on each capacitor is given by

$$q_A(t) = \frac{q_0}{2} \left(1 + e^{-\gamma t/2} \left(\cos(\omega_1 t) + \frac{\gamma}{2\omega_1} \sin(\omega_1 t) \right) \right) \quad (2)$$

$$q_B(t) = \frac{q_0}{2} \left(1 - e^{-\gamma t/2} \left(\cos(\omega_1 t) + \frac{\gamma}{2\omega_1} \sin(\omega_1 t) \right) \right) \quad (3)$$

In equations 2 and 3: $\omega_0^2 = \frac{1}{LC}$, $\gamma = \frac{R}{L}$, and $\omega_1^2 = \omega_0^2 - 4\gamma^2$. In experiment the site capacitances are about 815 pF and the coupling inductances are about 10 μ H. Since the bond switching time intimately depends on ω_1 (which itself depends on R through the γ^2 term), R needs to be on the order of 100 Ω to make ω_1 significantly different from ω_0 . The equivalent series resistance of the coupling inductors is only on the order of 1 Ω , so we are in the limit where $\omega_0 \gg \gamma$. Consequently, equations 2 and 3 drastically simplify to:

$$q_A(t) = \frac{q_0}{2} (1 + \cos(\omega_0 t)) \quad (4)$$

$$q_B(t) = \frac{q_0}{2} (1 - \cos(\omega_0 t)) \quad (5)$$

From equations 4 and 5, we can quickly find that the bond switching time is $\pi\sqrt{LC}$. Knowing this characteristic time, we can determine exactly how to modulate the coupling inductors.

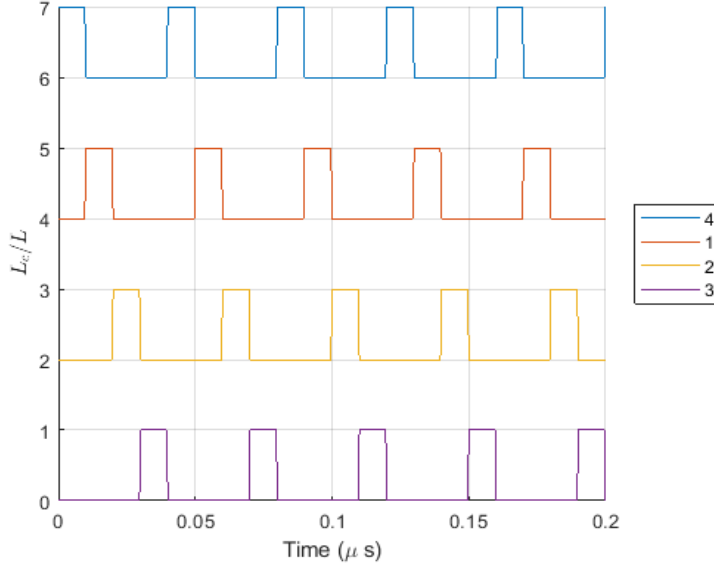


Figure 4: This plot shows how the inverse inductance of the coupling inductors is modulated as a square wave. The four curves plotted are vertically offset so that the periodic behaviors and phase differences of the four types of bonds can be easily seen. The curves are labeled according to the coupling inductor numbering notation established in Figure 2a. On the vertical axis is the ratio of the coupling inductance L to a reference inductance L_c . When the ratio L_c/L is 1 the coupling inductance is L_c , but when the ratio L_c/L is 0 the coupling inductance is infinite. This infinite inductance models a bond that does not allow adjacent sites to interact.

Figure 4 shows how the inductance varies in time for each of the four different types of coupling inductors. Inverse inductance is plotted on the vertical axis because inverse inductance is what appears in the equations of motion (Appendix B). The period of the square wave is four times the bond switching time so that four different types of bond switching can occur within one cycle. The duty cycle is 25% so that each type of bond only allows interaction for one bond switching period. With this bond switching scheme in place to produce

circulation, we can move forward to simulate the entirety of circuit one.

ii Solving the Entire Lattice Circuit

To solve the entire lattice circuit, we need set up the equations of motion that account for how all of the sites interact with each other. Since there will be a large number of equations to describe circuit one, it is useful to develop a notation that encapsulates information about where sites and bonds are in the lattice. We need to consider what the general A and B sites look like and to which inductors they are connected. Figure 5 shows an arbitrary A and B site, their connecting inductors, and the indexing notation that we use to identify where the sites and inductors are. Establishing this indexing notation has great utility in setting up the equations of motion and converting those equations of motion into a matrix equation (Appendix B).

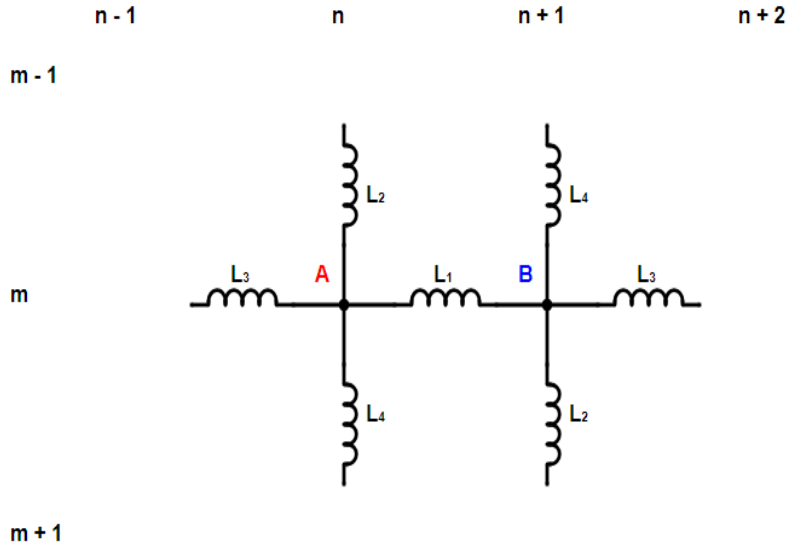


Figure 5: Above is a general A and B site with their corresponding coupling inductors. m and n index the rows and columns of the lattice.

I developed code that would solve the first order differential matrix equation for any size of lattice and for square wave modulated coupling inductors. Figure 6 shows a voltage plot which demonstrates successful circulation in a 6 by 6 lattice circuit. For that specific simulation, a voltage pulse of 1 V was initiated

on the site (1, 1). The first important thing to note is that this plot only shows the voltages on the sites on the $n = 1$ column of the lattice. Though the rest of 30 voltage signals are not shown, they are all approximately 0 during this time sample. The initialized voltage pulse travels down the left edge of the lattice, and none of the voltage leaks to bulk sites in the lattice. The voltage pulse travels by exchanging between two sites during a bond switching period, and the voltage exchanges how equations 4 and 5 predict. As the pulse travels along the edge, there are times when the voltage remains at a site for a switching period. This is simply because there are two bond switching periods between two opposing bonds on an edge site.

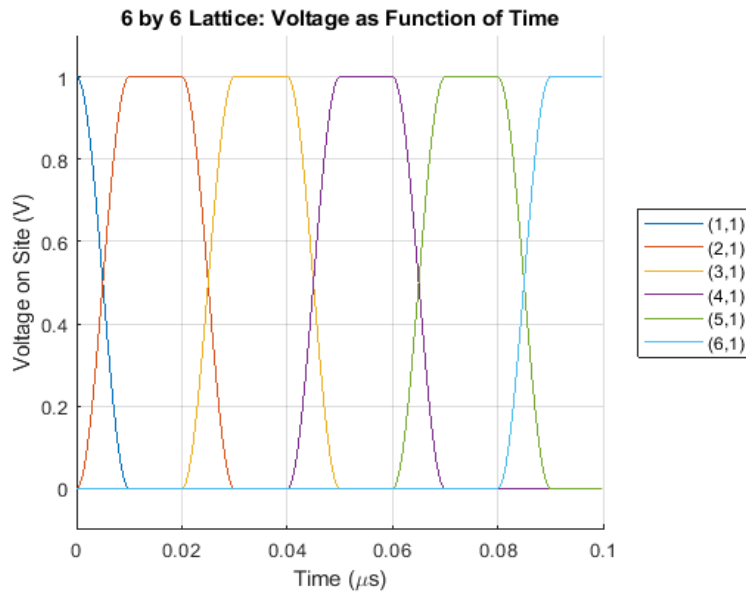


Figure 6: This plot shows the voltage as a function of time from the six sites on the left edge of a 6 by 6 lattice where 1 V is initialized on the site (1,1). Though not shown in this figure, a similar pattern persists for the voltage on the edge sites as the initial voltage pulse travels around the lattice counterclockwise.

Having success with this simulation, we proceeded to implement this model in a real circuit. Ultimately we decided that our best option to switch the bonds in the circuit was a frequency mixer. The SRA-6+ frequency mixer we chose does not operate properly unless its incoming and outgoing signals are above a threshold frequency of 3 kHz (Appendix D). When implementing the bond

switching in circuit one with mixers, the charge initialization produces a DC signal (i.e. 0 Hz signal) into the mixers. Since this is not above the threshold frequency of operation, we cannot create circuit one with these mixers as the bond switching mechanisms.

To circumnavigate this problem, we adjusted the sites of the lattice by adding an inductor in parallel to each site capacitor. When we initialize charge on a site capacitor, the voltage on the site will oscillate because the capacitor and inductor in parallel act as an oscillator. Since these oscillations occur on the order of 1 MHz, the mixers can operate as intended. This allows us to effectively use the mixers as our bond switching mechanism at the cost of slightly modifying the circuit one. And even though we are modifying the original circuit, we still expect to see the same qualitative result of non-reciprocity even if the quantitative details are different. Before, the unit cell was itself an oscillator in which the charge would exchange between the two site capacitors. Now, the unit cell consists of two oscillators that are coupled with an inductor. From classical mechanics we know that coupled oscillators can exhibit the behavior where the energy in one oscillator transfers to the other oscillator. Since we expect to see energy transfer between sites, we can also expect circulation to arise if the bond switching time is properly chosen.

B Circuit Two: Lattice Circuit with Sites as Capacitors and Inductors in Parallel

The new lattice circuit, hereafter referred to as circuit two, is identical in every respect to circuit one except that it has an inductor in parallel with the site capacitor. Figure 7 shows what the lattice looks like and what the new A and B sites look like. It is essential that we understand how the energy in the unit cell of the lattice behaves so that we can implement accurate bond switching times.

i Solving the Unit Cell of the Lattice Circuit

The unit cell of circuit two, depicted in Figure 8, consists of a capacitor and inductor in parallel inductively coupled to another capacitor and inductor in parallel. The site capacitors have capacitance C and charges q_A and q_B . The site inductors each have inductances L . The coupling inductor has inductance L_c and a current i_c flowing through it. The initial conditions for the circuit are that one of the capacitors is initially charged with some charge q_0 while the

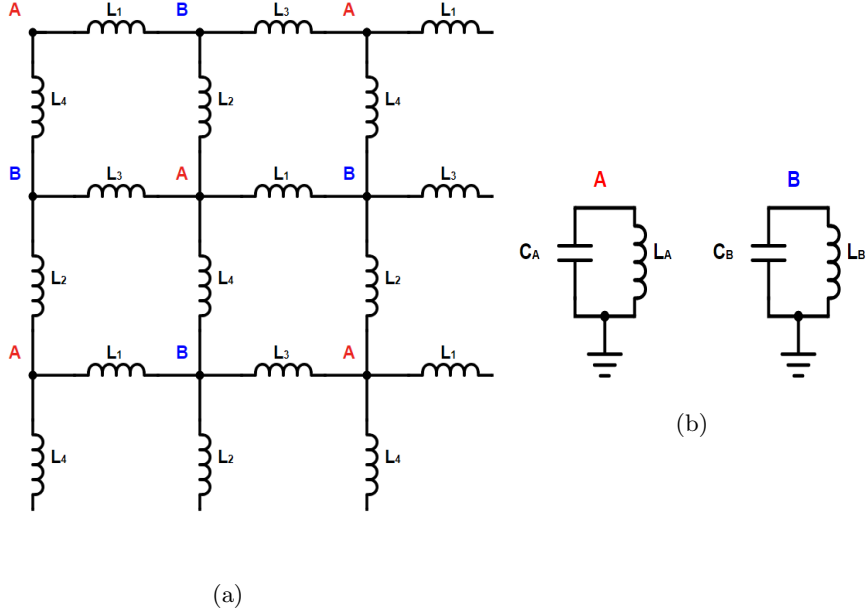


Figure 7: (a) This is a circuit diagram for circuit two. Each node in the circuit is a lattice site (A or B), and the sites are connected to each other by coupling inductors with inductances L_1 , L_2 , L_3 , and L_4 . (b) The A and B sites are capacitors and inductors that are connected in parallel and to ground. The capacitors have capacitances C_A and C_B , and the inductors have inductances L_A and L_B .

other capacitor is initially uncharged. Appendix C details the derivation of the solution to this circuit using Lagrangian mechanics and normal mode analysis. In this problem, it becomes useful to define a dimensionless coupling parameter $\alpha = \frac{L_c}{L}$, where L_c is the coupling inductance and L is the inductance of the site inductor. In the end, the normal frequencies and the solutions for the charge on each capacitor as functions of time are given by:

$$\omega_1 = \sqrt{\frac{1}{LC}} \qquad \omega_2 = \sqrt{1 + \frac{2}{\alpha}} \sqrt{\frac{1}{LC}} \qquad (6)$$

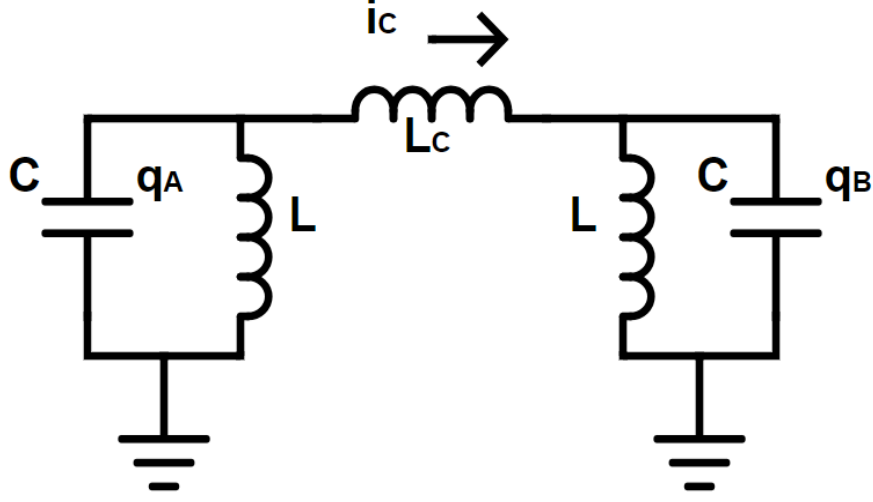


Figure 8: This is the circuit diagram for the unit cell of circuit two. The site capacitors have capacitance C and respective charge q_A and q_B . The site inductors each have inductance L . The coupling inductor has inductance L_c and a current i_c flowing through it.

$$q_A(t) = \frac{q_0}{2} \left(\cos(\omega_1 t) + \cos \left(\sqrt{1 + \frac{2}{\alpha}} \omega_1 t \right) \right) \quad (7)$$

$$q_B(t) = \frac{q_0}{2} \left(\cos(\omega_1 t) - \cos \left(\sqrt{1 + \frac{2}{\alpha}} \omega_1 t \right) \right) \quad (8)$$

$$i_c(t) = -\frac{\omega_1 q_0}{\sqrt{\alpha(\alpha + 2)}} \sin \left(\sqrt{1 + \frac{2}{\alpha}} \omega_1 t \right) \quad (9)$$

$$i_A(t) = \frac{\omega_1 q_0}{2} \left(\sin(\omega_1 t) + \sqrt{\frac{\alpha}{\alpha + 2}} \sin \left(\sqrt{1 + \frac{2}{\alpha}} \omega_1 t \right) \right) \quad (10)$$

$$i_B(t) = \frac{\omega_1 q_0}{2} \left(-\sin(\omega_1 t) + \sqrt{\frac{\alpha}{\alpha + 2}} \sin \left(\sqrt{1 + \frac{2}{\alpha}} \omega_1 t \right) \right) \quad (11)$$

Equation 6 defines the normal frequencies and equations 7 - 11 show how the charge and current in the circuit evolve in time. We want to know when all of the energy from one site has transferred to another site. More specifically, we want to know when $q_A = i_c = i_A = i_B = 0$ and $|q_B| = q_0$. We want these conditions to be true so that we reproduce the initial conditions of the circuit (i.e. only

charge on one capacitor and no current flowing in the circuit). Appendix D provides a derivation for the conditions under which this can happen. A full energy transfer can only happen for particular values of α :

$$\alpha = \frac{-2(2m + n + 1)^2}{(1 + 2m)(2m + 2n + 1)} \quad (12)$$

In equation 12, $m, n \in \mathbb{Z}$ and are independent of each other. Since $\alpha > 0$, we also require constraints on what m and n can be. If $m \leq -1$, then $n > -m$; if $m \geq 0$, then $n < -m$. Once we have selected valid options for m and n , the time at which energy fully transfers is given by:

$$t = \frac{1}{\omega_1} ((2m + n + 1)\pi + 2\pi k) \quad (13)$$

In this equation, k is an arbitrary integer. The smallest magnitudes of m and n that will produce a valid α are $m = 0$ and $n = -2$, which result in $\alpha = \frac{2}{3}$ and the first nonnegative $t = \pi\sqrt{LC}$. Now that we know the relationship between the site and coupling inductors and the corresponding bond switching time, we can model a lattice circuit that will exhibit full energy transfer between its sites.

ii Solving a 2 by 2 Circuit

In the previous chapter I simulated circuit one using MATLAB scripts, but to simulate circuit two, I used LTspice, an electronic circuit simulator. Figure 9 shows circulation in a 2 by 2 version of circuit two in which a pulse initiated at site (1,1) travels counterclockwise around the circuit. During the first bond switching period, which lasts about 282 ns, the voltage transfers from (1,1) to (2,1). In the next bond switching period the voltage transfers from (2,1) to (2,2). This pattern continues as the voltage travels counterclockwise around the circuit.

From the plot, we can see that the voltage on a site is almost always zero unless there is voltage transferring to it from a previous site or unless it is transferring voltage to the next site. Therefore, the voltage on a site is only nonzero during two consecutive bond switching periods. Unlike the bond switching technique used for circuit one, there are no prolonged periods of time when the voltage stays at a site. Additionally, we can see that there are small fluctuations around 0 V after 1 μ s. Some reasons why these small fluctuations are present are because the resistive switching mechanism used by LTspice cannot perfectly switch between zero and infinite ohms, and because the bond switching may not have quite precise enough timing.

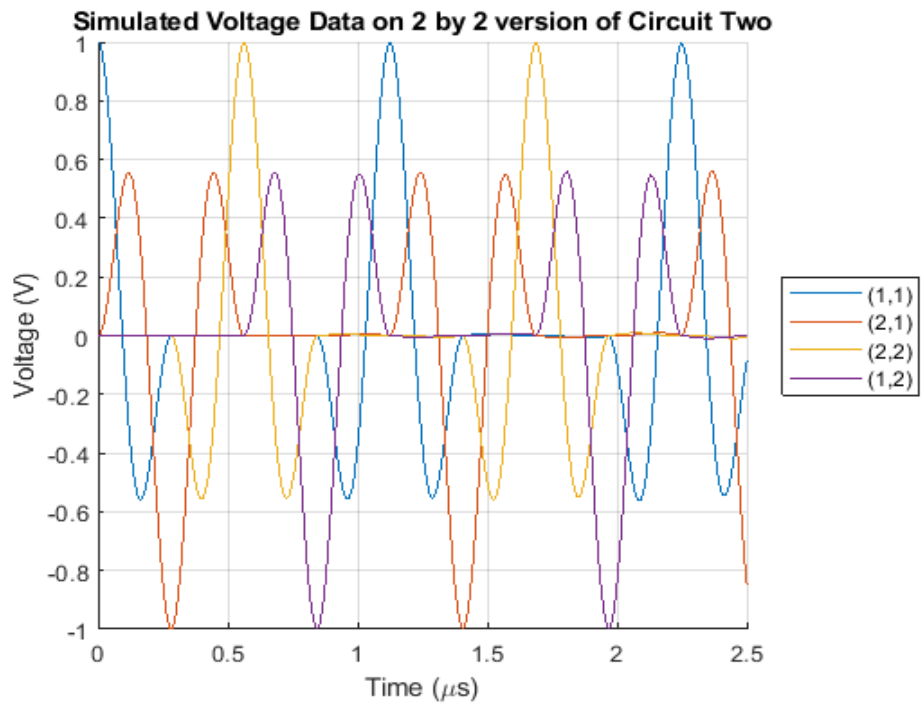


Figure 9: This is the voltage plot for a simulated 2 by 2 version of circuit two. The voltage pulse here travels counterclockwise around the circuit. After 1 μ s has passed, we can see slight deviations arise because the voltage on some sites is nonzero when it should ideally be zero.

3 Experiment

A Testing the Unit Cell for Circuit Two

Since $\alpha = 2$ cannot be written of the form given by equation 12, then there is no time when all of the energy from one site will transfer to another. However, we can still determine an optimal switching time by observing voltage data from a unit cell for circuit two without any switching. We used a model for the capacitor voltages given by equations 7 and 8 in addition to voltage data from a circuit described in Figure 8. Figure 10 shows the simulated and measured voltages on each capacitor in the unit cell of circuit two.

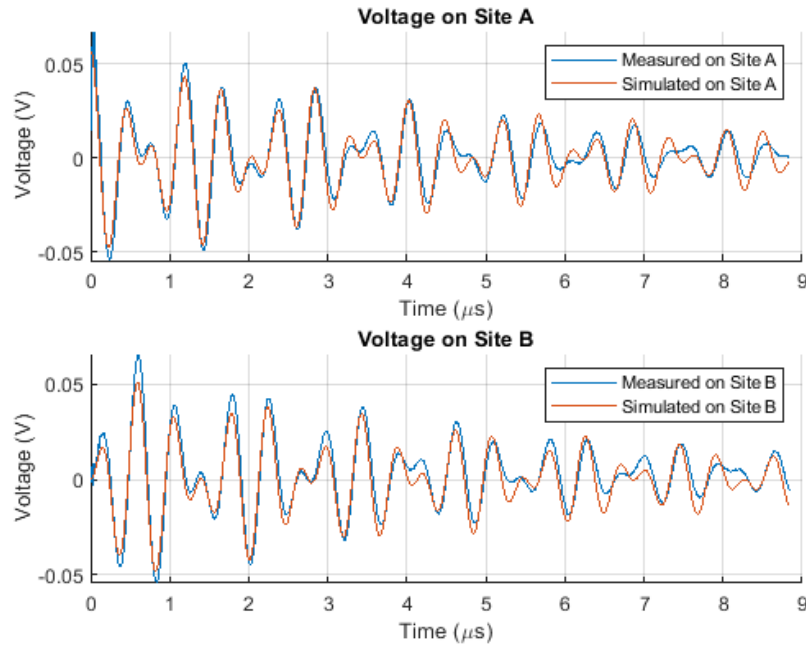


Figure 10: This plot shows simulated and measured voltages on sites A and B of the unit cell of circuit two ($\alpha = 2$). There is no bond switching either in the simulation or in the experiment. In the simulation and in the experiment, there is a voltage pulse initialized on site A while there is no voltage initialized on site B .

The simulation curves are not exactly the same as equations 7 and 8, since I added in a simple exponential decay term to model the decay that I observed in

the data. The model agrees well with the data and we can thus use our model to determine the optimal bond switching time. This optimal bond switching time turns out to be about 600 ns.

B Experimental Setup for 2 by 2 Version of Circuit Two

Knowing the bond switching time allows us to attempt to produce circulation in a lattice circuit. Figure 11 shows the circuit diagram for the 2 by 2 lattice that I constructed. In the four quadrants of the diagram, you can see the four sites of the lattice. Each site is a capacitor and inductor in parallel and connected to ground. The A and B sites alternate throughout the lattice, and the bonds connecting all of them are shown as a switch between two coupling inductors. All of the switches are in fact connected to bias lines because these switches actually represent mixers which require bias lines that turn the bonds on and off.

Two important parts of this circuit that are not present in my previous discussions of the circuit two are the voltage initialization and the presence of only two bias lines. In the top right corner, there is a voltage source that provides a voltage pulse across a small capacitor and across a site. The purpose of the small capacitor is to help impart a small amount of charge to the larger capacitor in the site without the small capacitor and voltage source affecting the site throughout the rest of the experiment. At a given frequency, the impedance of a small capacitor is larger than the impedance of a large capacitor, and it is this large impedance that helps isolate the small capacitor and voltage source from the rest of the circuit.

Next, this circuit diagram only shows two bias lines, while my model presumed that each type of inductor had a different type of switching. Even in the 2 by 2 version of circuit two there is still one of each type of inductor, so it seems that we need four bias lines instead of the two shown. The 2 by 2 case is special, though, because each site cannot be connected to more than two other sites. If opposing bonds (i.e. 1 and 3, 2 and 4) receive the same switching signals but the two signals are π out of phase, then there is no time during which a site can be connected to two bonds. Even though the 2 by 2 version of circuit two has four different types of inductors, the circuit only requires two bias lines to properly switch the bonds.

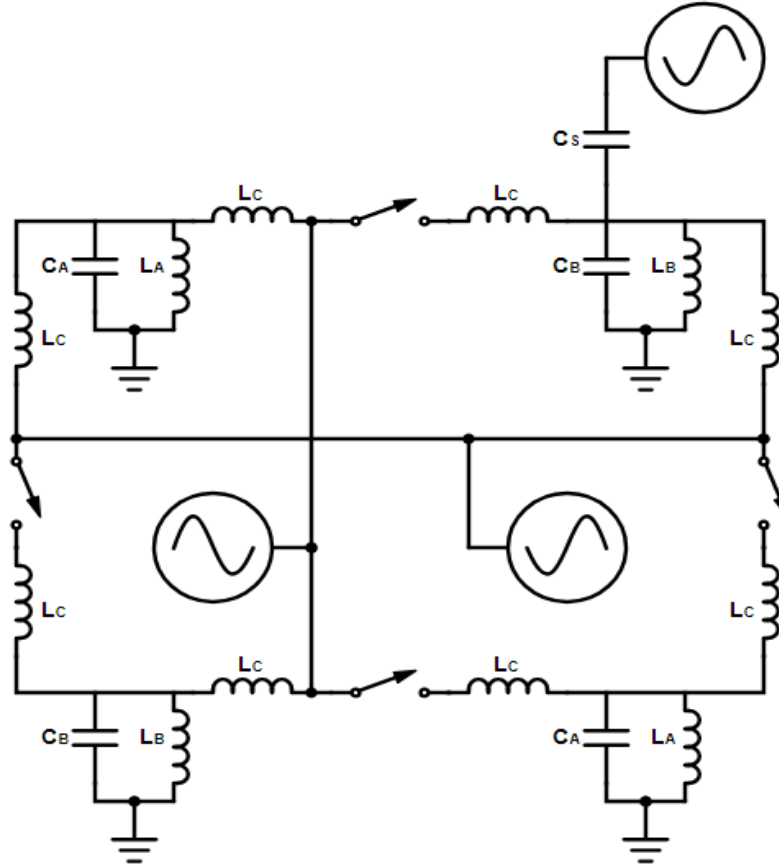


Figure 11: This is a circuit diagram for a 2 by 2 version of circuit two. There are four sites in the four quadrants of the diagram, and they alternate between A and B sites. Their capacitances are $C_A = C_B \approx 815$ pF. Their inductances are $L_A = L_B \approx 10\mu\text{H}$. Between each site are two coupling inductors each one with inductance L_c , though the value of L_c depends on the coupling parameter α that we want to investigate. The voltage signal in the top right initializes a voltage on the capacitor in the top right site via a small capacitor with $C_s \approx 80$ pF. The voltage signals shown in the middle of the circuit each output a bias signal to a pair of opposing mixers that are represented by switches.

Figure 12 is a picture of the physical circuit that I used for the 2 by 2 lattice with $\alpha = 2$. The inductors and blue capacitors in the four corners of the circuit are the four sites of the lattice. The four metallic, rectangular devices are the

mixers and the inductors on either side of each mixer are the coupling inductors. To each mixer is attached a bias line, and each pair of opposing mixers shares a bias line. The bias lines connect to function generators which provide the square wave switching of the bonds. In the top right corner is the small yellow capacitor that, in combination with the voltage pulse provided by the purple and black wire, initializes voltage on the top right site. The voltage pulse is created by a third function generator. Located on the outside of the circuit are four scope probes that are connected to an oscilloscope which reads off the voltage at each site.

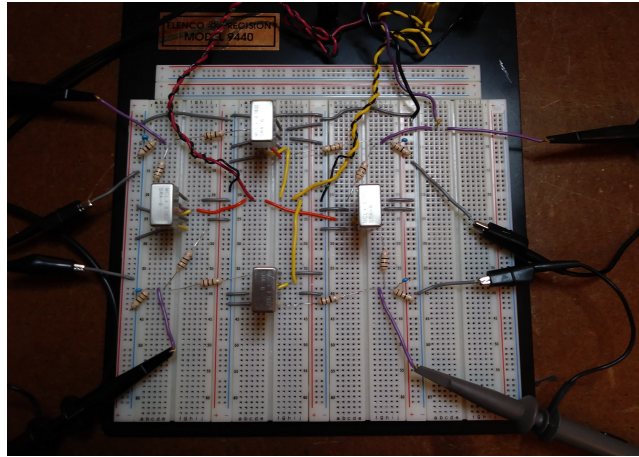


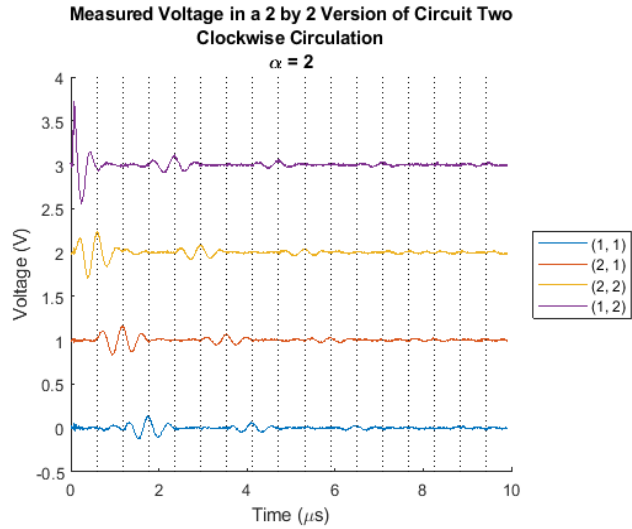
Figure 12: This is a picture of the 2 by 2 version of circuit two that I assembled on a prototyping board. The site capacitors are the small blue capacitors in each quadrant of the board, and they are connected in parallel with tan inductors. The sites are all connected to each other with two tan inductors in between which are frequency mixers (silver metal boxes). The circuit shown is for the case $\alpha = 2$ since every inductor shown has the same value and there are two coupling inductors in series for each site inductor. In the top right corner is a small yellow capacitor connected to a purple and black twisted pair that delivers the initializing voltage pulse. The orange/yellow and black twisted pairs connect to the frequency mixers and provide the two unique biasing signals. There are also four scope probes situated at each site to measure the voltage on the capacitors in time.

C Testing a 2 by 2 Version of Circuit Two for Non-Reciprocity

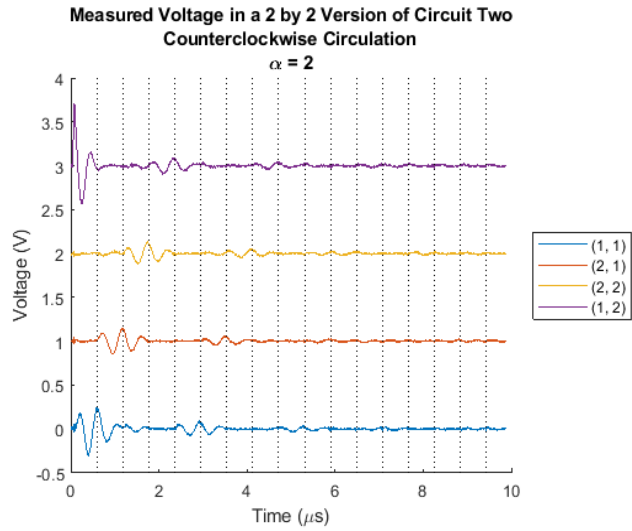
Using the circuit shown in Figure 12, I tested it to see if I could observe non-reciprocity for both $\alpha = 2$ and $\alpha = \frac{2}{3}$. The capacitors in the circuit had capacitances $C_A = C_B \approx 815$ pF and $C_s \approx 80$ pF. The site inductors in the circuit had inductances $L_A = L_B \approx 10\mu\text{H}$. The coupling inductors were either about $10\ \mu\text{H}$ or $3.33\ \mu\text{H}$ depending on if $\alpha = 2$ or $\alpha = \frac{2}{3}$. The bias lines were square waves with twice the period of the bond switching period, and the delay time between the two bias lines is one bond switching period. Figures 13 and 14 show that non-reciprocity does arise from the lattice circuit under these conditions. From those figures, though, we can see that the circulation appears stronger when $\alpha = 2$. Stronger circulation means that the voltage at the site is very close to 0 unless it is transferring voltage, and it means that the voltage pulse travels several times around the lattice before decaying to 0. The circulation in Figure 13 is clearly stronger than the circulation in 14 using this definition.

The voltages on each site of the lattice are plotted as a function of time and are vertically offset so that the voltage pulses can be seen more clearly. The dashed lines on the plots show every time either of the mixers switches on or off. Focusing on Figure 13a, we can see that during the first switching period, the voltage transfers from (1, 2) to (2, 2). In the proceeding switching periods, we notice the same pattern in which the voltage from one site transfers to the site adjacent in the clockwise direction. Notably, the voltage on the sites is 0 unless it is connected with a site that has nonzero voltage or unless it is transferring voltage to an adjacent site. Furthermore, the voltage pulse can travel around the lattice in the exact opposite direction just by changing the delay time between the two bias lines (Figure 13b).

An important aspect of both plots is the decay of the voltage pulse as it travels around the circuit. The pulse only travels around the circuit one to three times before its amplitude is too small to discern from the noise around 0 V. The decay likely originates from a combination of the equivalent series resistance of the coupling inductors and from the loss in the mixers. More precisely understanding the nature of the loss is crucial to testing non-reciprocity in larger versions of circuit two in the future.



(a)



(b)

Figure 13: Both of these graphs plot the measured voltage on the site capacitors of the 2 by 2 version of circuit two. In these plots, $\alpha = 2$. The dashed lines show when either of the mixers switches a bond on or off. The voltages are vertically offset so that the voltage pulses on each site can more clearly be distinguished. In both cases there is a voltage pulse initialized at the site (1,2). (a) In this plot, the voltage pulse travels around the circuit clockwise. (b) In this plot, the voltage pulse travels around the circuit counterclockwise.

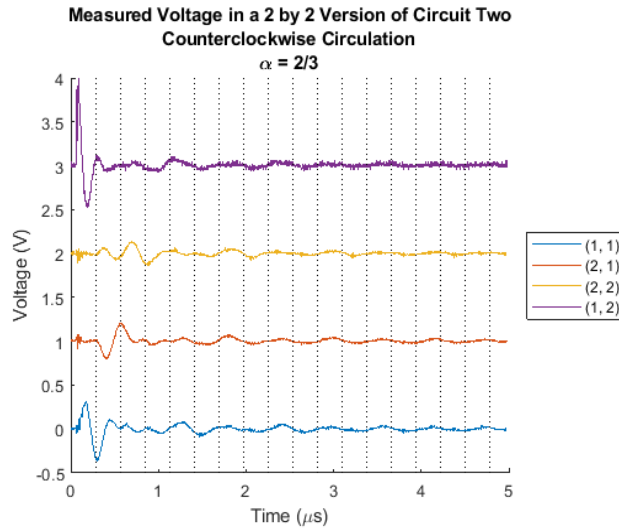
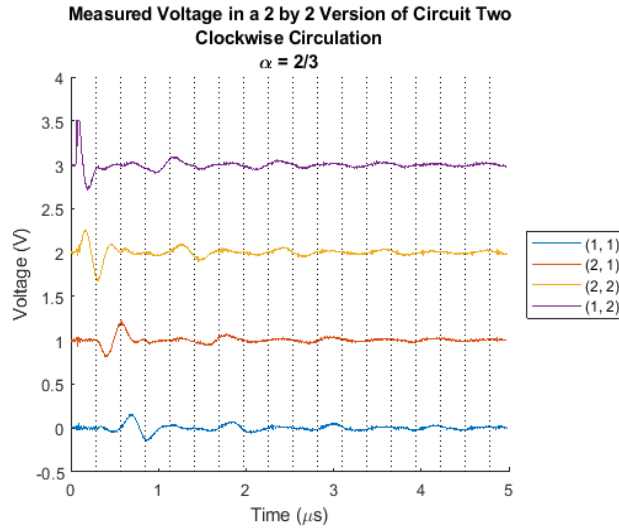


Figure 14: Both of these graphs plot the measured voltage on the site capacitors of the 2 by 2 version of circuit two. In these plots, $\alpha = \frac{2}{3}$. The dashed lines show when either of the mixers switches a bond on or off. The voltages are vertically offset so that the voltage pulses on each site can more clearly be distinguished. In both cases there is a voltage pulse initialized at the site (1,2). (a) In this plot, the voltage pulse travels around the circuit clockwise. (b) In this plot, the voltage pulse travels around the circuit counterclockwise.

I also executed simulations of the two 2 by 2 versions of circuit two with different values of α . Figures 15 and 16 show the simulated and measured data on each site in the circuit. The simulated data have been modified by simple decaying exponentials to model the measured decay. The simulations and measurements agree well in the shapes of the voltage curves that they produce; however, the simulations do not model the amplitude of the voltage signal as well. This is likely the case because a simple exponential decay does not accurately model dissipation in the circuit, but instead a more complicated decay model is needed.

One last thing to note about the simulated and measured data shown in Figures 15 and 16 is that the data for $\alpha = 2$ produce better circulation than the data for $\alpha = \frac{2}{3}$. This is perhaps unexpected since we showed in the section on solving the unit cell of circuit two that we obtain full energy transfer for $\alpha = \frac{2}{3}$ but not for $\alpha = 2$. One possible resolution is that the full energy transfer at $\alpha = \frac{2}{3}$ is unstable to small variations in the values of the circuit components. It could be the case that small variations in capacitance and inductance (which are impossible to fully eliminate) produce large variations in how voltage transfers when $\alpha = \frac{2}{3}$, but the $\alpha = 2$ case is more resilient to variations in component values. Even though $\alpha = \frac{2}{3}$ may theoretically be an optimal coupling strength, in practice more stable circulation may be achieved using different values of α that still have significant, if not full, energy transfer.

Simulated and Measured Voltages on 2 by 2 Version of Circuit Two
 $\alpha = 2$

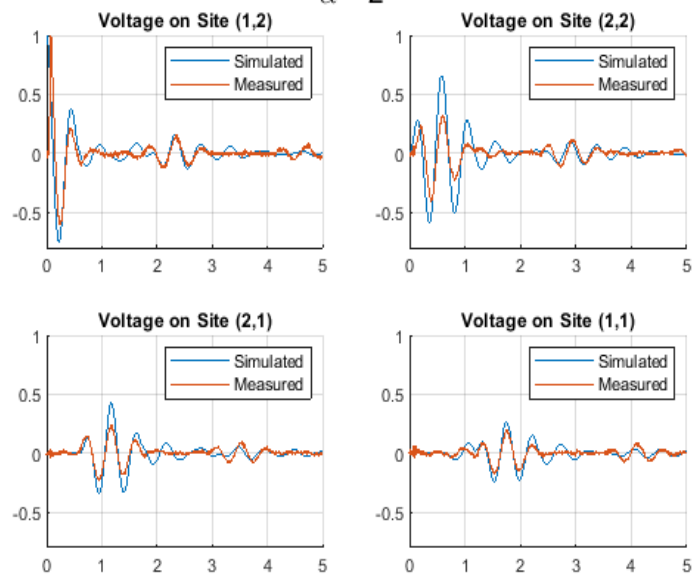


Figure 15: The above four plots show the simulated and measured voltages on each site in the 2 by 2 version of circuit two with $\alpha = 2$.

Simulated and Measured Voltages on 2 by 2 Version of Circuit Two
 $\alpha = 2/3$

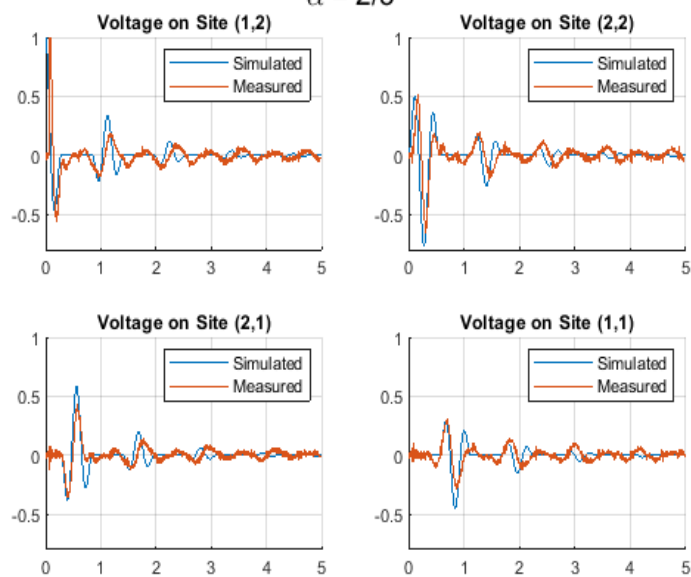


Figure 16: The above four plots show the simulated and measured voltages on each site in the 2 by 2 version of circuit two with $\alpha = \frac{2}{3}$.

4 Conclusion

One of my main research goals was to design and perform tests on a circuit to see if it could exhibit non-reciprocity like a chip-scale circulator should. Rudner's discussion of a time-dependent lattice circuit that exhibits non-reciprocity inspired us to design a two-dimensional lattice circuit which produces circulation. My experimental data shown in Figures 13 and 14 demonstrate that I have successfully created a non-reciprocal circuit. My simulated data shown in Figures 15 and 16 demonstrate that I have a successful model to describe how a lattice circuit with bond switching evolves in time.

In my future work, I want to deeper analyze how the coupling parameter α affects energy transfer and the stability of that energy transfer. The data suggest that there may be stability issues in energy transfer between sites when α has a value that produces optimal energy transfer. I also want to acquire a better understanding of the voltage decay in the 2 by 2 version of circuit two. Understanding what causes the rapid voltage decay is imperative before I can proceed to test larger versions of circuit two because I need to be able to detect signals after many bond switching periods. After addressing the decay problem, I can proceed to test if larger versions of circuit two experience bulk excitations during circulation. The results of this will be interesting to compare to the claims made in Rudner's paper about large lattices with defects on the boundary. Finally, if further tests of circuit two confirm that it is a viable option to use as a circulator, then I will work to create a superconducting version of the circuit. There are many future directions I can go with this project now that I have successfully produced non-reciprocity in a 2 by 2 lattice circuit.

5 Appendix

A Circuit One: Solution to Unit Cell

This simple circuit shown in Figure 3 is the unit cell of the lattice circuit. Given capacitors with capacitances C and an inductor with inductance L and equivalent series resistance R , the corresponding equation of motion given by Kirchoff's voltage law is:

$$\frac{1}{C}q_A + R\dot{q}_A + L\ddot{q}_A - \frac{1}{C}q_B = 0$$

Now in the lattice circuit, the initial conditions are $q_A(0) = q_0$ and $q_B(0) = 0$, where q_0 is some charge initialized on the capacitor. Implicit in the above equation is the fact that $\dot{q}_A = -\dot{q}_B$, which must hold by conservation of charge. Integrating both sides yields $q_A + q_B = c_0$, where c_0 is a constant. This relation holds for all time, and thus holds for $t = 0$, which implies that $q_A + q_B = q_0$. Now the differential equation can be written in terms of only one variable:

$$\ddot{q}_A + \frac{R}{L}\dot{q}_A + \frac{1}{LC}q_A = \frac{q_0}{LC} \quad (1)$$

The solutions to this differential equation are well understood. After making the appropriate substitutions, the solutions for $q_A(t)$ and $q_B(t)$ are given by:

$$\omega_0^2 = \frac{1}{LC} \quad \gamma = \frac{R}{L} \quad \omega_1^2 = \omega_0^2 - 4\gamma^2$$

$$q_A(t) = \frac{q_0}{2} \left(1 + e^{-\gamma t/2} \left(\cos(\omega_1 t) + \frac{\gamma}{2\omega_1} \sin(\omega_1 t) \right) \right) \quad (2)$$

$$q_B(t) = \frac{q_0}{2} \left(1 - e^{-\gamma t/2} \left(\cos(\omega_1 t) + \frac{\gamma}{2\omega_1} \sin(\omega_1 t) \right) \right) \quad (3)$$

Using the approximations $\gamma \ll \omega_0$ and $\gamma t \ll 1$, the solutions simplify to:

$$q_A(t) = \frac{q_0}{2} (1 + \cos(\omega_0 t)) \quad (4)$$

$$q_B(t) = \frac{q_0}{2} (1 - \cos(\omega_0 t)) \quad (5)$$

B Circuit One: Equations of Motion

Using the index notation shown in Figure 5, I first set up equations for Kirchoff's current and voltage laws that apply for a general site. The first two equations ensure that Kirchoff's current laws are satisfied, and the last four equations ensure that Kirchoff's voltage laws are satisfied. Importantly, I use the convention where positive current flow is defined to be in the direction of increasing m and n . In the equations below, v refers to the voltage on a site with respect to ground and its subscript identifies the site as an A site or a B site. Their superscripts denote the position of the site on the indexed grid (Figure 5). The i refers to the current flowing in the coupling inductor between two sites and its subscript identifies it as one of the four types of inductors in the lattice. Their superscripts denote into which site the current is flowing. The constants C and L are the capacitance and inductance of the circuit elements, and their subscripts denote the site type (A, B) or inductor type (1, 2, 3, 4).

$$\begin{aligned}
\frac{d}{dt} v_A^{m,n} &= \frac{1}{C_A} \left(i_2^{m,n} + i_3^{m,n} - i_1^{m,n+1} - i_4^{m+1,n} \right) \\
\frac{d}{dt} v_B^{m,n+1} &= \frac{1}{C_B} \left(i_1^{m,n+1} + i_4^{m,n+1} - i_2^{m+1,n+1} - i_3^{m,n+2} \right) \\
\frac{d}{dt} i_1^{m,n+1} &= \frac{1}{L_1} \left(v_A^{m,n} - v_B^{m,n+1} \right) \\
\frac{d}{dt} i_2^{m,n} &= \frac{1}{L_2} \left(v_B^{m-1,n} - v_A^{m,n} \right) \\
\frac{d}{dt} i_3^{m,n} &= \frac{1}{L_3} \left(v_B^{m,n-1} - v_A^{m,n} \right) \\
\frac{d}{dt} i_4^{m+1,n} &= \frac{1}{L_4} \left(v_A^{m,n} - v_B^{m+1,n} \right)
\end{aligned}$$

Now this system of differential equations can be rewritten as a matrix equation. To write consolidate the system of equations into one matrix equation, I utilized the following vectors: \vec{v} , \vec{i} , and \vec{v} .

$$\vec{v} = \begin{pmatrix} v_1 \\ v_2 \\ \vdots \\ v_{MN} \end{pmatrix} \quad \vec{i} = \begin{pmatrix} i_A \\ i_B \\ \vdots \\ i_{2MN-M-N} \end{pmatrix} \quad \vec{v} = \begin{pmatrix} \vec{v} \\ \vec{i} \end{pmatrix} \quad \vec{\mu} = \frac{d}{dt} \begin{pmatrix} \vec{v} \\ \vec{i} \end{pmatrix}$$

At this point, it is important to note that I am defining the lattice size to be $M \times N$. Given a lattice of that size, there will be MN sites and there will

be $2MN - M - N$ coupling inductors. Next, I need to define the dynamical matrix which will control how the components of \vec{v} interact with each other. The dynamical matrix D can be compartmentalized into four submatrices called D_1 , D_2 , D_3 , and D_4 .

$$D = \begin{pmatrix} D_1 & D_2 \\ D_3 & D_4 \end{pmatrix}$$

It makes sense to consider these submatrices independently because each one controls a different relationship between v , $\frac{dv}{dt}$, i , and $\frac{di}{dt}$. D_1 controls how $\frac{dv}{dt}$ and v relate, and terms in this submatrix arise from time dependent capacitors or resistors in parallel with the capacitors. D_2 controls how $\frac{dv}{dt}$ and i relate, and terms in this submatrix arise from current flowing through the coupling inductors. D_3 controls how $\frac{di}{dt}$ and v relate, and terms in this submatrix arise from the presence of capacitors connecting to the coupling inductors. Finally, D_4 controls how $\frac{di}{dt}$ and i relate, and terms in this submatrix arise from time dependent inductors or resistors in series with the coupling inductors. Now we can write down a first-order differential matrix equation that MATLAB can more easily solve than systems of higher-order differential equations.

$$\frac{d}{dt}\vec{v} = D\vec{v}$$

C Circuit Two: Solution to Unit Cell

The circuit is shown in Figure 8 and is the unit cell of the lattice circuit with sites that are a capacitor and an inductor in parallel. The inductors on the sites have inductance L , the capacitors on the sites have capacitance C , and the coupling inductor has inductance L_c . Positive current flows through the circuit clockwise, and the currents through the sites' inductors and the coupling inductor are i_A , i_B , and i_c respectively. The solution to this circuit can be found by constructing the appropriate Lagrangian:

$$\mathcal{L} = \frac{1}{2}Li_A^2 + \frac{1}{2}Li_B^2 + \frac{1}{2}L_c i_c^2 - \frac{1}{2C}q_A^2 - \frac{1}{2C}q_B^2$$

This Lagrangian can be written in terms of only three coordinates by using the constraints that $i_A = i_c - \dot{q}_A$ and $i_B = i_c + \dot{q}_B$. Now we have a final Lagrangian and its three corresponding Euler-Lagrange equations.

$$\mathcal{L} = \frac{1}{2}l(i_c - q_A)^2 + \frac{1}{2}l(i_c + q_B)^2 + \frac{1}{2}L_c i_c^2 - \frac{1}{2C}q_A^2 - \frac{1}{2C}q_B^2$$

$$\frac{d}{dt} \left(\frac{\partial \mathcal{L}}{\partial \dot{i}_c} \right) = \frac{\partial \mathcal{L}}{\partial i_c} \quad \frac{d}{dt} \left(\frac{\partial \mathcal{L}}{\partial \dot{q}_A} \right) = \frac{\partial \mathcal{L}}{\partial q_A} \quad \frac{d}{dt} \left(\frac{\partial \mathcal{L}}{\partial \dot{q}_B} \right) = \frac{\partial \mathcal{L}}{\partial q_B}$$

$$\left(2 + \frac{L_c}{L} \right) \dot{i}_c = \dot{q}_A - \dot{q}_B \quad L(\dot{i}_c - \dot{q}_A) = \frac{1}{C}q_A \quad L(\dot{i}_c + \dot{q}_B) = -\frac{1}{C}q_B$$

Defining $\alpha = \frac{L_c}{L}$, and eliminating i_c , we obtain a system of equations for q_A and q_B .

$$\begin{aligned} \left(1 - \frac{1}{\alpha + 2} \right) \ddot{q}_A + \frac{1}{\alpha + 2} \ddot{q}_B &= -\frac{1}{LC}q_A \\ \left(1 - \frac{1}{\alpha + 2} \right) \ddot{q}_B + \frac{1}{\alpha + 2} \ddot{q}_A &= -\frac{1}{LC}q_B \end{aligned}$$

Rewriting this equation as a matrix equation, we obtain:

$$\begin{pmatrix} 1 - \frac{1}{\alpha + 2} & \frac{1}{\alpha + 2} \\ \frac{1}{\alpha + 2} & 1 - \frac{1}{\alpha + 2} \end{pmatrix} \begin{pmatrix} \ddot{q}_A \\ \ddot{q}_B \end{pmatrix} = - \begin{pmatrix} \frac{1}{LC} & 0 \\ 0 & \frac{1}{LC} \end{pmatrix} \begin{pmatrix} q_A \\ q_B \end{pmatrix}$$

Solving this as a normal modes problem, the resulting normal frequencies are:

$$\omega_1 = \sqrt{\frac{1}{LC}} \quad \omega_2 = \sqrt{1 + \frac{2}{\alpha}} \sqrt{\frac{1}{LC}} \quad (6)$$

Finally, we need to apply the initial conditions: $q_A(0) = q_0$, $q_B(0) = 0$, $\dot{q}_A(0) = 0$, and $\dot{q}_B(0) = 0$. This results in the solution for the charges and currents in the circuit:

$$q_A(t) = \frac{q_0}{2} \left(\cos(\omega_1 t) + \cos \left(\sqrt{1 + \frac{2}{\alpha}} \omega_1 t \right) \right) \quad (7)$$

$$q_B(t) = \frac{q_0}{2} \left(\cos(\omega_1 t) - \cos \left(\sqrt{1 + \frac{2}{\alpha}} \omega_1 t \right) \right) \quad (8)$$

$$i_c(t) = -\frac{\omega_1 q_0}{\sqrt{\alpha(\alpha + 2)}} \sin \left(\sqrt{1 + \frac{2}{\alpha}} \omega_1 t \right) \quad (9)$$

$$i_A(t) = \frac{\omega_1 q_0}{2} \left(\sin(\omega_1 t) + \sqrt{\frac{\alpha}{\alpha + 2}} \sin \left(\sqrt{1 + \frac{2}{\alpha}} \omega_1 t \right) \right) \quad (10)$$

$$i_B(t) = \frac{\omega_1 q_0}{2} \left(-\sin(\omega_1 t) + \sqrt{\frac{\alpha}{\alpha + 2}} \sin \left(\sqrt{1 + \frac{2}{\alpha}} \omega_1 t \right) \right) \quad (11)$$

D Optimization of Coupling Parameter

In Appendix C, equations 7 - 11 demonstrate the solution to the unit cell of circuit two. However, it is important for us to know if there exist times when all of the energy from one site has transferred to the other site. Specifically, we want to know the time when all of the energy from the first site is solely in the capacitor of the next site. This ensures that the initial conditions are exactly reproduced, but the initial charge is on the opposite site. So, we require that $q_A = i_c = i_A = i_B = 0$ and $|q_B| = q_0$ at some time. Using the substitution $\theta = \omega_1 t$, the following four equations are what need to be solved to determine what α and θ can be:

$$\begin{aligned} \cos \theta + \cos \left(\sqrt{\frac{\alpha + 2}{\alpha}} \theta \right) &= 0 \\ \sin \left(\sqrt{\frac{\alpha + 2}{\alpha}} \theta \right) &= 0 \\ \sin \theta + \sqrt{\frac{\alpha}{\alpha + 2}} \sin \left(\sqrt{\frac{\alpha + 2}{\alpha}} \theta \right) &= 0 \\ -\sin \theta + \sqrt{\frac{\alpha}{\alpha + 2}} \sin \left(\sqrt{\frac{\alpha + 2}{\alpha}} \theta \right) &= 0 \end{aligned}$$

From these equations, we can derive two equations that constrain α and θ .

$$\left(1 - \sqrt{\frac{\alpha + 2}{\alpha}}\right) \theta = (2m + 1)\pi \quad \sqrt{\frac{\alpha + 2}{\alpha}} \theta = n\pi$$

In these equations, $m, n \in \mathbb{Z}$. After solving these equations for α and θ , we get the following results:

$$\alpha = \frac{-2(2m + n + 1)^2}{(1 + 2m)(2m + 2n + 1)} \quad (12)$$

$$\theta = (2m + n + 1)\pi + 2\pi k \quad (13)$$

To ensure that $\alpha \geq 0$, we require two conditions on m and n . If $m \leq -1$, then $n > -m$; if $m \geq 0$, then $n < -m$. Since θ is only determined up to 2π , there is a $2\pi k$ term ($k \in \mathbb{Z}$) to account for this ambiguity. Something very important to note is that there are strict conditions on what α and its corresponding θ can be. We have shown that for this system the coupling parameter must be written in the form given by equation 12. This means that for an arbitrary value of α there will not be a moment in time when all of the energy has transferred from one site to the next site.

E Datasheet for SRA-6+ Frequency Mixer

Plug-In Frequency Mixer

Level 7 (LO Power +7 dBm) 0.003 to 100 MHz

SRA-6+



CASE STYLE: A01

Maximum Ratings

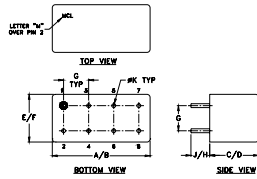
Operating Temperature -55°C to 100°C
 Storage Temperature -55°C to 100°C
 RF Power 50mW
 IF Current 40mA
 Permanent damage may occur if any of these limits are exceeded.

Pin Connections

LO	8
RF	1
IF	3,4 [^]
GROUND	2,5,6,7

[^] pins must be connected together externally

Outline Drawing



Outline Dimensions (inches)

A	B	C	D	E	F
.770	.800	.385	.400	.370	.400
19.56	20.32	9.78	10.16	9.40	10.16
G	H	J	K		wt
.200	.20	.14	.031		grams
5.08	5.08	3.56	0.79		5.2

Features

- excellent conversion loss, 4.58 dB typ.
- high L-R isolation, 45 dB typ. L-I isolation, 40 dB typ.
- rugged welded construction
- hermetic

Applications

- VHF TV
- defense & federal communications
- radio astronomy

+RoHS Compliant
 The +Suffix identifies RoHS Compliance. See our web site for RoHS Compliance methodologies and qualifications

Electrical Specifications

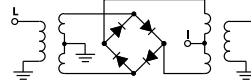
FREQUENCY (MHz)		CONVERSION LOSS (dB)			LO-RF ISOLATION (dB)				LO-IF ISOLATION (dB)								
LO/RF	IF	Mid-Band		Total	L		U		L		U						
f ₁ -f ₂		X	σ	Max.	Typ.	Min.	Typ.	Min.	Typ.	Min.	Typ.	Min.					
.003-100	DC-100	4.58	.05	7.5	8.5	60	50	45	30	35	25	60	45	40	25	30	20

1 dB COMP: +1 dBm typ. L = low range [f₁ to 10 f₁] M = mid range [10 f₁ to f₂/2] U = upper range [f₂/2 to f₂]
 σ = mid-band [f₁ to f₂]

Typical Performance Data

Frequency (MHz)	Conversion Loss (dB)		VSWR RF Port (-1)		Frequency (MHz)	Isolation L-R (dB)		Isolation L-I (dB)		VSWR LO Port (-1)
	LO	LO +7dBm	LO	LO +7dBm		LO	LO +7dBm	LO	LO +7dBm	
0.25	30.25	4.69	1.18		0.25	87.94	69.25	2.72		
0.50	30.50	4.70	1.21		0.50	88.51	67.15	2.60		
1.00	31.00	4.72	1.23		1.00	80.05	62.74	2.56		
2.00	32.00	4.71	1.23		2.00	74.49	58.28	2.48		
4.00	34.00	4.72	1.25		4.00	65.04	46.76	2.43		
6.00	36.00	4.75	1.26		6.00	61.86	45.54	2.42		
8.00	38.00	4.77	1.25		8.00	58.66	43.62	2.43		
10.00	40.00	4.77	1.24		10.00	62.82	41.15	2.44		
15.00	45.00	4.75	1.24		15.00	62.74	40.69	2.45		
19.00	49.00	4.72	1.23		19.00	59.34	40.12	2.47		
23.00	53.00	4.69	1.20		23.00	55.11	40.91	2.50		
31.00	61.00	5.04	1.19		31.00	51.93	41.11	2.55		
39.00	69.00	5.21	1.17		39.00	50.11	39.64	2.58		
51.00	81.00	5.29	1.22		51.00	48.56	38.35	2.62		
61.00	91.00	5.51	1.37		61.00	47.39	36.57	2.65		
67.00	97.00	5.71	1.44		67.00	45.06	33.06	2.70		
70.00	100.00	5.80	1.46		70.00	44.27	31.87	2.74		
85.00	115.00	5.84	1.41		85.00	43.62	30.32	2.89		
92.50	122.50	5.90	1.24		92.50	43.22	30.02	2.98		
100.00	130.00	5.93	1.12		100.00	42.87	30.05	3.06		

Electrical Schematic



Notes
 A. Performance and quality attributes and conditions not expressly stated in this specification document are intended to be excluded and do not form a part of this specification document.
 B. Electrical specifications and performance data contained in this specification document are based on Mini-Circuits' applicable established test performance criteria and measurement instructions.
 C. The parts covered by this specification document are subject to Mini-Circuits' standard limited warranty and terms and conditions (collectively, "Standard Terms"). Purchasers of this part are entitled to the rights and benefits contained therein. For a full statement of the Standard Terms and the exclusive rights and remedies thereunder, please visit Mini-Circuits' website at www.minicircuits.com/MCStore/terms.jsp



www.minicircuits.com P.O. Box 350166, Brooklyn, NY 11235-0033 (718) 934-4500 sales@minicircuits.com

REV B
 MINS107
 SRA-6+
 DUT/DIP/DM
 151005
 Page 1 of 2

References

- [1] Benjamin J. Chapman, Eric I. Rosenthal, Joseph Kerckhoff, Bradley A. Moores, Leila R. Vale, J.A.B. Mates, Gene C. Hilton, Kevin Lalumière, Alexandre Blais, and K.W. Lehnert *Phys. Rev. X* **7**, 041043 (2017)
- [2] Mark S. Rudner, Netanel H. Lindner, Erez Berg, and Michael Levin *Phys. Rev. X* **3**, 031005 (2013)